Pharm Res (2012) 29:83–96
DOI 10.1007/s11095-011-0513-7

RESEARCH PAPER

Self-Assembled Polymersomes Conjugated with Lactoferrin as Novel Drug Carrier for Brain Delivery

Yuan Yu • Zhiqing Pang • Wei Lu • Qi Yin • Huile Gao • Xinguo Jiang

Received: 17 March 2011 / Accepted: 10 June 2011 / Published online: 7 October 2011

ABSTRACT

Purpose To develop a novel brain drug delivery system based on self-assembled poly(ethyleneglycol)-poly (D,L-lactic-co-glycolic acid) (PEG-PLGA) polymersomes conjugated with lactoferrin (Lf-POS). The brain delivery properties of Lf-POS were investigated and optimized.

Method Three formulations of Lf-POS, with different densities of lactoferrin on the surface of polymersomes, were prepared and characterized. The brain delivery properties in mice were investigated using 6-coumarin as a fluorescent probe loaded in Lf-POS (6-coumarin-Lf-POS). A neuroprotective peptide, S14G-humanin, was incorporated into Lf-POS (SHN-Lf-POS); a protective effect on the hippocampuses of rats treated by Amyloid-$\beta_{25\text{-}35}$ was investigated by immunohistochemical analysis.

Results The results of brain delivery in mice demonstrated that the optimized number of lactoferrin conjugated per polymersome was 101. This obtains the greatest blood–brain barrier (BBB) permeability surface area(*PS*) product and percentage of injected dose per gram brain (%ID/g brain). Immunohistochemistry revealed the SHN-Lf-POS had a protective effect on neurons of rats by attenuating the expression of Bax and caspase-3 positive cells. Meanwhile, the activity of choline acetyltransferase (ChAT) had been increased compared with negative controls.

Conclusion These results suggest that lactoferrin functionalized self-assembled PEG-PLGA polymersomes could be a promising brain-targeting peptide drug delivery system via intravenous administration.

KEY WORDS BBB · brain delivery · lactoferrin · peptide · polymersomes

Y. Yu
Department of Pharmaceutics, School of Pharmacy
The Second Military Medical University
800 Xiangyin Road
Shanghai 200433, China

Z. Pang • W. Lu • Q. Yin • H. Gao • X. Jiang
Department of Pharmaceutics, School of Pharmacy, Fudan University
826 Zhangheng Road
Shanghai 201203, China

Z. Pang • W. Lu • Q. Yin • H. Gao • X. Jiang (✉)
Key Laboratory of Smart Drug Delivery Ministry of Education & PLA
P. R. 826 Zhangheng Road
Shanghai 201203, China
e-mail: xgjiang@shmu.edu.cn

INTRODUCTION

A significant challenge for 21st century medicine is to positively affect the clinical outcomes that follow debilitating central nervous system (CNS) diseases linked to aging, infections and degeneration. These include, but are not limited to Alzheimer's and Parkinson's diseases, stroke, amyotrophic lateral sclerosis, multiple sclerosis and HIV-1-associated neurocognitive disorders. The development of neuroscience facilitated the discovery of macromolecular drugs, including peptides, recombinant proteins, monoclonal antibodies, and gene therapies, with considerable potential. Macromolecular drugs may be particularly useful to treat these types of CNS diseases because they reach novel targets with a high specificity (1). However, the blood-brain barrier (BBB) represents an insurmountable obstacle for almost 100% of therapeutic macromolecules. Therefore, it is very important to develop novel drug delivery systems with brain-targeting features to improve the efficacy of macromolecular drugs in the treatment of CNS diseases (2). One current

candidate is receptors-mediated targeting via intravenous injection of ligand-conjugated drug delivery systems that target to receptors expressed on the luminal side of the BBB (2–6). Well-characterized BBB receptors mainly include the following: low-densities lipoprotein receptor (LDLR), transferrin receptor (7–9), epidermal growth factor receptor and insulin-like growth factor receptor (3,10). As a single-chain iron-binding glycoprotein, lactoferrin is a multifunctional protein to which several physiological roles have been attributed. The multiple biological activities of lactoferrin are mediated by receptors (11). Several lines of evidence, including the results of immuno-histochemistry and reverse transcriptase-polymerase chain reaction (RT-PCR), have indicated the presence of specific lactoferrin receptors in the brain. Ji *et al.* (12) revealed that the distribution volume of I125-labeled lactoferrin in rat brain tissue was 2.2 times that of transferrin and twice that of OX26, indicating the possibility of lactoferrin as a brain-targeting ligand.

Colloidal systems, such as liposomes and polymer-based nanoparticles, have shown promise as drug carriers to target the brain after intravenous administration. Colloidal carriers presented great potential for drug targeting, including optimization of a drug's pharmacokinetics in the bloodstream, protection of drugs against inactivation and premature activity en route to the target (13–15). This advantage of colloidal carriers has been attributed to the so-called enhanced permeability and retention (EPR) effect (15). Discher and Eisenberg (16) proposed a new concept of "self-assemble of block copolymers," referring to the fact that since the diblock copolymers are thermodynamically incompatible, they can be self-assembled to supramolecular aggregates with specific shapes in a solvent system. A member of this group, polymersomes, i.e., polymer vesicles, has received great interest in recent years (16,24,36). It has been shown that polymersomes can be formed from synthetic amphiphilic block copolymers using organic solvent, organic solvent/water systems, or aqueous media (16). Polymersomes are promising in biomedical applications, such as artificial cells, and also for mimicking cell membranes (17). However, exploration of polymersomes as drug delivery systems has been minimally reported. With a similar structure to the liposomes, polymersomes are 30–200 nm in linear size and are made up of an aqueous intracavity and a bilayer membrane. Copolymers forming bilayers in aqueous media provide capsular vehicles, the internal aqueous space of which can be used for delivery of hydrophilic drugs, while the copolymer aggregates bilayer can be loaded with small hydrophobic drugs (17–19). Additionally, the membrane of polymersomes is thicker than that of liposomes (~10 nm compared to ~3 nm), providing highly durable carriers that are able to resist the deforming forces that destroy liposomes. Therefore, they can be used for encapsulation of guest molecules as well as controlled and sustained release.

Humanin, discovered by Mamiya, is a neuroprotective peptide that serves to specifically block Alzheimer's diseases (AD)-related apoptosis, and it is the solitary linear oligopeptide that can inhibit the neurotoxic effect induced both by amyloid-β and by FAD gene mutation. S14G-humanin, derived from humanin, in which the 14th amino acid serine is substituted by glycine, is 1,000 times more potent than humanin when tested *in vitro*. (20) However, its potential therapeutic applications are limited by its susceptibility to peptidases and poor passage across the BBB via intravenous administration.

The purpose of the current work was to prepare and evaluate the *in vivo* brain delivery properties, after intravenous administration, of polymersomes as a drug carrier, where lactoferrin was conjugated to the surface of polymersomes (Lf-POS) with different densities. Block copolymer poly(ethyleneglycol)-poly(D,L-lactic-co-glycolic acid) (PEG-PLGA) was used for preparing polymersomes due to its favorable biodegradability. In addition, 6-coumarin, a lipophilic green fluorescent dye, was incorporated into Lf-POS as a vesicle probe. The pharmacokinetic profiles of Lf-POS were investigated to estimate the brain transport properties of Lf-POS. Furthermore, S14G-humanin peptide was encapsulated into Lf-POS and presented neuroprotective effects to rats via intravenous administration.

MATERIALS AND METHODS

Materials

Lactoferrin, 6-coumarin and rabbit anti-goat immunoglobulin (IgG) gold (10 nm) conjugate were purchased from Sigma-Aldrich (St. Louis, USA). S14G-humanin was obtained from the Chinese Peptide Company (Hangzhou, China). Bovine lactoferrin ELISA quantitation kit was purchased from the Bethyl Laboratories (Montgomery, USA). Methoxy-PEG (MW 3,000 Da) was purchased from NOF Corporation (Tokyo, Japan). D,L-lactide and glycolide were purchased from PURAC (Gorinchem, Netherlands). Mouse anti-rat CD 68 polyclonal antibody was purchased from Serotec Ltd. (Oxford, UK). Maleimide-PEG (MW 3,500 Da) was purchased from Jenkem Technology Corporation (Beijing, China). Rabbit anti-Bax polyclonal antibody (sc-526) was purchased from Santa Cruz Biotechnology, Inc. (Santa Cruz, USA). Rabbit anti-caspase3 polyclonal antibody (ab2302) was purchased from Abcam (Cambridge, USA). Rabbit anti-choline acetyltransferase polyclonal antibody (BA0596) was purchased from Boster Biological (Wuhan, China). Double-distilled water was purified using a Millipore Simplicity

System (Millipore, Bedford, USA). All the other chemicals were analytical reagent grades and used without further purification. Kunming mice, BALB/c mice (♂weighing 20–22 g) and Sprague-Dawley rats (SD rats) (♂weighing 180–220 g) were obtained from Shanghai SLAC Laboratory Animal Co. Ltd. (Shanghai, China).

All animal experiments were carried out according to guidelines approved and evaluated by the ethical committee of Fudan University.

Copolymer Synthesis and Characterization

The diblock copolymer of methoxy-PEG-PLGA and maleimide-PEG-PLGA were synthesized by the ring-opening polymerization of D,L-lactide and glycolide in the presence of PEGmer as initiators and using stannous octoate as catalyst (21). In brief, a predetermined amount of methoxy-PEG or maleimide-PEG, D,L-lactide and glycolide in a bottle-neck flask were heated to 140°C, under nitrogen atmosphere, for complete melting. After melting the reactants, stannous octoate (0.5%, w/w) was dissolved in toluene and added to the reaction mixture as a catalyst. The flask was evacuated under vacuum for 1 h and then sealed. Then the polymerization was carried out at 130°C for 24 h. After the completion of the reaction, the copolymers were purified by dissolving them in chloroform, followed by precipitation in ice-cold ether. The precipitated copolymers were filtered and dried under vacuum at 40°C for 24 h and then stored in a desiccator under vacuum. The number average molecular weight (Mn) and the composition of the copolymers were investigatived by ^{1}H-NMR and ^{13}C-NMR using $CDCl_3$ as the solvent (21,26).

Preparation of Polymersomes

Polymersomes were prepared using a self-assembly method in which acetone was utilized as the water-miscible organic solvent. In a typical procedure (18), a blend of methoxy-PEG-PLGA and maleimide-PEG-PLGA was dissolved in 1 ml of acetone to a concentration of 6 mg/ml, and then the mixture was injected into 5 ml PBS (0.01 M, pH7.4) with the tip of the syringe immersed close to the bottom of the bottle. Mild stirring was executed, and this induced POS by self-assembly at room temperature. After 4 h, the solution was dialyzed to remove the organic solvent using dialysis membranes (3,500 Da).

A similar preparation method for polymersomes loaded with 6-coumarin (6-coumarin-POS) was utilized, with approximately 100 μg of 6-coumarin added to the mixture organic solution of copolymer. The polymersomes were eluted and purified by a Sepharose CL-4B column.

The S14G-humanin peptide was actively encapsulated in polymersomes using a pH gradient method (22–24). Briefly, a blend of maleimide-PEG-PLGA and methoxy-PEG-PLGA was dissolved in 1 ml of acetone, slowly injected into 5 ml $(NH_4)_2SO_4$ solution (120 mM) and then left to stand for 4 h. After 4 h, the solution was dialyzed to remove acetone using dialysis membranes (3,500 Da). Polymersomes were concentrated, and the $(NH_4)_2SO_4$ solution was exchanged with 0.1 M NaCl solution using a concentrator tube. Then 0.5 ml of S14G-humanin solution (1 mg/ml) and 100 μl 1,4-dioxine were added into the polymersomes solution and incubated at 37°C for 30 min. The polymersomes was purified as described above.

Lactoferrin-functionalized polymersomes (Lf-POS) were formed according to the methods described previously (25,26). Briefly, lactoferrin was thiolated using 2-iminothiolane with a 60:1 molar ratio. After letting the reaction proceed for 60 min, the sulfhydrylated lactoferrin was incubated and slowly stirred with polymersomes for 6 h under nitrogen atmosphere away from light. The molar ratio of sulfhydrylated lactoferrin to maleimide was 1:1. Following conjugation, Lf-POS were purified with a Sepharose CL-4B column and eluted with PBS (0.01 M, pH7.4).

Characterization of Polymersomes

The properties of polymersomes were characterized using dynamic light scattering (DLS) to give size and zeta potential (NICOMP^{TM} 380 ZLS; PSS, USA). The morphological appearance of Lf-POS was observed by transmission electron microscope (TEM) (CM120; Philips, Netherlands) and cryogenic transmission electron microscopy (cryo-TEM) (JEOL 2010; JEOL, Japan). In brief, thin films (approximately 100-250 nm) of 1.0 wt% Lf-POS in water were suspended in a microperforated grid and rapidly vitrified using liquid ethane (-183°C), until it was loaded into a cryogenic sample holder. Images were observed with a JEOL2010 TEM at 200 kV combined with Gatan832CCD imager using a resolution of 0.3 nm focus for improved digital recording (19). To confirm the surface-conjugation of lactoferrin to polymersomes, immuno-gold staining was performed. Briefly, Lf-POS was consecutively incubated with an anti-lactoferrin primary antibody and then a 10 nm colloidal gold-labeled secondary antibody.

Calculation of the Lactoferrin Densities on the Surface of Lf-POS

According to a previous study, the densities of ligand modified on the surface of vesicles had a direct impact on the plasma clearance and brain targeting of the nanoparticles (25,27). Therefore, ELISA was performed (28) to measure the surface lactoferrin concentrations of Lf-POS (A, ng/ml) using a bovine lactoferrin quantitation kit. The

average lactoferrin molecules conjugated per milliliter in the equivalent elution fractions (M) was calculated as: $M = A \times 10^{-9} \times 6.02 \times 10^{23}/(MW \times V)$. The molecular weight of lactoferrin (MW) was 83,100 Da. The concentration of Lf-POS (C, mg/ml) was calculated by the turbidimetry measurements at 350 nm using UV spectrophotometer (UV2401; Shimadzu, Japan). The average number of Lf-POS per milliliter elution fractions (N) was calculated with following equation: $N = \frac{6 \times C \times 10^{-3}}{\pi \times (D^3 - r^3) \times 10^{-7} \times \rho}$, $\rho = 1.1$ g/cm^3, where D was the linear size of Lf-POS, and r was the inside cavity diameter of Lf-POS, which was calculated using the following equation: r = D-2 d, where d was the membrane thickness of polymersomes obtained by cryo-TEM. Therefore, the average number of lactoferrin conjugated per polymersomes was calculated by dividing M by N.

X-ray Photoelectron Spectroscopy (XPS)

To further show the surface modification, chemical composition of the surface layer was determined before and after treating the conjugation by using X-ray photoelectron spectroscopy (XPS). POS, Lf-POS and the physical mixture of maleimide-PEG-PLGA, methoxy-PEG-PLGA (1:5), were all analyzed to determine the surface composition of C, O and N as previously described (26,29).

Drug Loading and Release *in Vitro*

According to previous studies (26,30), the drug loading efficiency (DLE) of either 6-coumain or S14G-humanin in Lf-POS was measured with HPLC associated with the turbidimetry method. The accumulated release of either 6-coumarin or S14G-humanin from polymersomes *in vitro* was processed with 1.0 ml of 6-coumarin-Lf-POS or S14G-humanin-Lf-POS, incubated in a dialysis bag (MW 12 kDa,) and submerged in 10 ml PBS (pH 7.4 or 4.0) at 37°C under slow agitation. At varying time points, the cumulative release percentage (CR_t) was calculated. During the experiment, the samples were kept away from light.

$$DLE(\%) = \frac{\text{drug concentration in polymersomes solution}}{\text{polymersomes concentration in the same solution}} \times 100\%$$

In Vivo Pharmacokinetics and Tissue Distribution of Lf-POS Loaded with 6-coumarin

The brain transport property of Lf-POS with different surface lactoferrin densities was evaluated. Pharmacokinetics and tissue distribution studies were performed (25,26). 6-coumarin, green fluorescence probe was encapsulated into the following experimental formulations with different lactoferrin densities, from low to high: 6-coumarin-Lf_{59}-POS, 6-coumarin-Lf_{101}-POS and 6-coumarin-Lf_{268}-POS. One hundred male Kunming mice, weighing 20-22 g, were randomly divided into four groups. The animals were injected with either experimental formulations or 6-coumarin-POS at a dose of 4 mg/kg via tail vein. At 0.03, 0.08, 0.25, 0.5 and 1 h following i.v. injection, the blood sample and the main organs, including brain, heart, liver, spleen, lung and kidney, were collected and treated with cold saline to remove blood ($n = 5$ for each time point).

The blood and tissue samples were extracted and reconstituted as described in our previous works (26), and RP-HPLC was performed on the samples. Pharmacokinetic parameters were calculated using a statistical moment analysis according to the noncompartmental model of blood drug concentrations (percent injected dose (%ID) per ml blood). The tissue volume of distribution (V_D) of a sample, at a given time point after i.v. injection, was determined from the ratio of drug in a tissue (%ID per g of tissue) divided by the concentration of the drug (%ID/ml) in the terminal plasma. The brain permeability surface area (*PS*) product was determined as follows: $PS = \frac{[V_D - V_0]Cp(T)}{\int_0^t Cp(t)dt}$, where Cp(T) = the terminal blood concentration and V_0 = the brain volume distribution of a blood volume marker. Based on the method reported by Huwyler (25) and Lu (26) *et al.*, the brain V_D of polymersomes was used as a plasma volume marker (V_0) for the calculation of brain *PS* products. V_0 was defined as the brain volume distribution and was determined by the amount of polymersomes in the brain tissue (%ID per g tissue) divided by the plasma concentration of polymersomes (%ID/ml) at 2 min after i.v. injection. Brain uptake was indicated as %ID per g of brain tissue and calculated as follows: $\%ID/g(t) = PS \times AUC_{0-t}$.

Immunohistochemical Staining for CD68

To evaluate the acute inflammatory reaction and cytotoxic cellular responses caused by Lf-POS, BALB/c mice (♂ weighing 20-22 g) were injected with Lf-POS at a dose of 150 mg/kg/day for 7 days. Twenty four h and 72 h after the last injection, the animals were fixed in 4% paraformaldehyde solution, and the cerebrum, cerebellum, heart, lung, liver, spleen and kidney were collected, embedded into paraffin and cut into 5 μm sections. All sections were subsequently stained with a mouse monoclonal CD68 antibody (1:100 dilutions) overnight at 4°C. Sections were developed using 3,3′-diaminobensidine (DAB) and stained with hematoxylin (31,32).

Immunohistochemical Analysis of Lf-POS Loaded with S14G-humanins

The amyloid-$\beta_{25\text{-}35}$ was dissolved in water and prepared into a 2 g/l solution; amyloid-$\beta_{25\text{-}35}$ was sealed and shaken

at 37°C for 76 h to make condensed amyloid-$\beta_{25\text{-}35}$ (33,34). SD rats were anesthetized with 20% urethane (800 mg/kg, intraperitoneal injection) and wrapped on a stereotaxic apparatus. Their anterior fontanelle was exposed using a cranial median incision. Taking the anterior fontanelle as the original point, the skull was drilled 3.0 mm behind it and 2.0 mm left and right to original point using a #7 needle. After the needle was vertically inserted along the skull into the brain tissue for 3.2 mm, 5μl of condensed amyloid-$\beta_{25\text{-}35}$ (2 g/l) was slowly injected into the bilateral hippocampuses. The needle remained for 5 min before it was slowly removed and the incision was closed. The sham controls were injected with the same volume of normal saline.

Subsequent to the operation, the SD rats were randomized into 3 groups (n=8, each). The experimental group was administrated SHN-Lf_{101}-POS with a dosage of S14G-humanin (25 μg/kg), sham control group (saline was injected into the bilateral hippocampuses instead of Amyloid-$\beta_{25\text{-}35}$) and negative control group (administration of saline, 1.2 ml/kg). Fourteen days post operation, the animals were given the test formulations for 12 continuous days via intravenous injection. After the 12 days of continuous administration, anesthetized rats were perfused with transcardiac perfusion (0.9% NaCl followed by 4% paraformaldehyde). After paraffin embedding, about 5 mm brain tissue around the amyloid-$\beta_{25\text{-}35}$ injection site was sampled. Five μm coronal sections, with 100 μm intervals, were prepared. The samples were subsequently dewaxed in xylene and washed sequentially in 100, 90, and 70% ethanol and finally in PBS (0.01 M, pH7.4). Immunohistochemical analysis was performed with rabbit anti-ChAT polyclonal antibody (1:1,000 dilution), rabbit anti-Bax polyclonal antibody (1:1,000 dilution) or rabbit anti-ChAT polyclonal antibody (1:1,000 dilution) overnight at 4°C, respectively. Slides were then rinsed and incubated with VECTASTAIN®ABC kits. To visualize positive signals, slides were developed with 3,3′-diaminobensidine (DAB) and counter-stained with hematoxylin. The positive cells around the amyloid-$\beta_{25\text{-}35}$ injection region were observed.

Data were expressed as mean ± S.E.M. Statistical analysis was performed by one-way ANOVA or independent sample t-test. A P value<0.05 was regarded as statistically significant. All of the statistical analyses were performed using SPSS 11.5 software.

RESULTS

Copolymer Synthesis and Characterization

The chemical reactions for the prepartion of PEG-PLGA are shown in Fig. 1e. The molecular weight (Mw) and the composition of the copolymers were analyzed by ^{1}H-NMR and ^{13}C-NMR using $CDCl_3$ as a solvent (Fig. 1). The integrals of the peaks at 1.57 ppm(^{1}H) and 16.67 ppm (^{13}C) corresponded to the LA methyl group (–CH_3). The peaks at 5.21 ppm (^{1}H) and 69.85 ppm (^{13}C) corresponded to the LA methine proton (-CH-). The peaks at 4.78 ppm (^{1}H) and 61.62 ppm (^{13}C) corresponded to the GA methene group (-CH_2-). The methene group (-CH_2-) of PEG appeared at 3.65 (^{1}H) and 71.55 ppm (^{13}C). The peaks at 166.26 ppm (^{13}C) and 170.15 ppm (^{13}C) were attributed to the carbonyl carbons (-C = O) of LA and GA, respectively. The molecular weight ratio of PLGA to PEG was based on the PEG methylene protons (δ3.65 ppm). The peak that corresponded to the maleimide proton (δ6.65 ppm) was utilized to prove the presence of the maleimide group in the copolymer. According to the ^{1}H ratio of the peak areas at 5.21, 4.78 and 3.65 ppm, the average molecular weight ratios of maleimide-PEG to PLGA and methoxy-PEG to PLGA were calculated to be 3,500:10,180 and 3,000:9,042, respectively. The LA/GA composition was 75:25.

Characterization of Polymersomes

The average size of the polymersomes and Lf-POS was approximately 90 nm and 120 nm, respectively (Table I). After binding lactoferrin, the diameter of Lf-POS increased slightly and showed a consistent size and zeta potential. The zeta potential values of both Lf-POS and polymersomes were approximately –4mv (Table I). Lf-POS were slightly larger and more positive in zeta potential than polymersomes. The difference in zeta potential is presumably due to the positive charge of the lactoferrin N-terminal fragment. Lf-POS exhibited nanosphere and consistent sizes when examined by TEM (Fig. 2b). Cryo-TEM indicated that the Lf-POS were hollow vesicles with an obvious outer membrane structured by an amphipathic copolymer (Fig.2a). The membranes that yielded polymersomes had a thickness of 10 nm. Immune colloidal gold labeling resulted in the black gold particles being bound to the outer membrane of Lf-POS. This suggested that lactoferrin bound itself to the secondary antibody labeled with the colloidal gold via the primary antibody, which demonstrated the conjugation between lactoferrin and Lf-POS (Fig. 2c). The numbers of lactoferrin conjugated per polymersomes a listed in Table I. Three types of Lf-POS, each with a different surface lactoferrin densities, were prepared (from 59 to 268).

In Vitro Drug Loading and Release

The DLE of 6-coumarin loaded into polymersomes was approximately 0.25%, which is sufficient for qualitative and

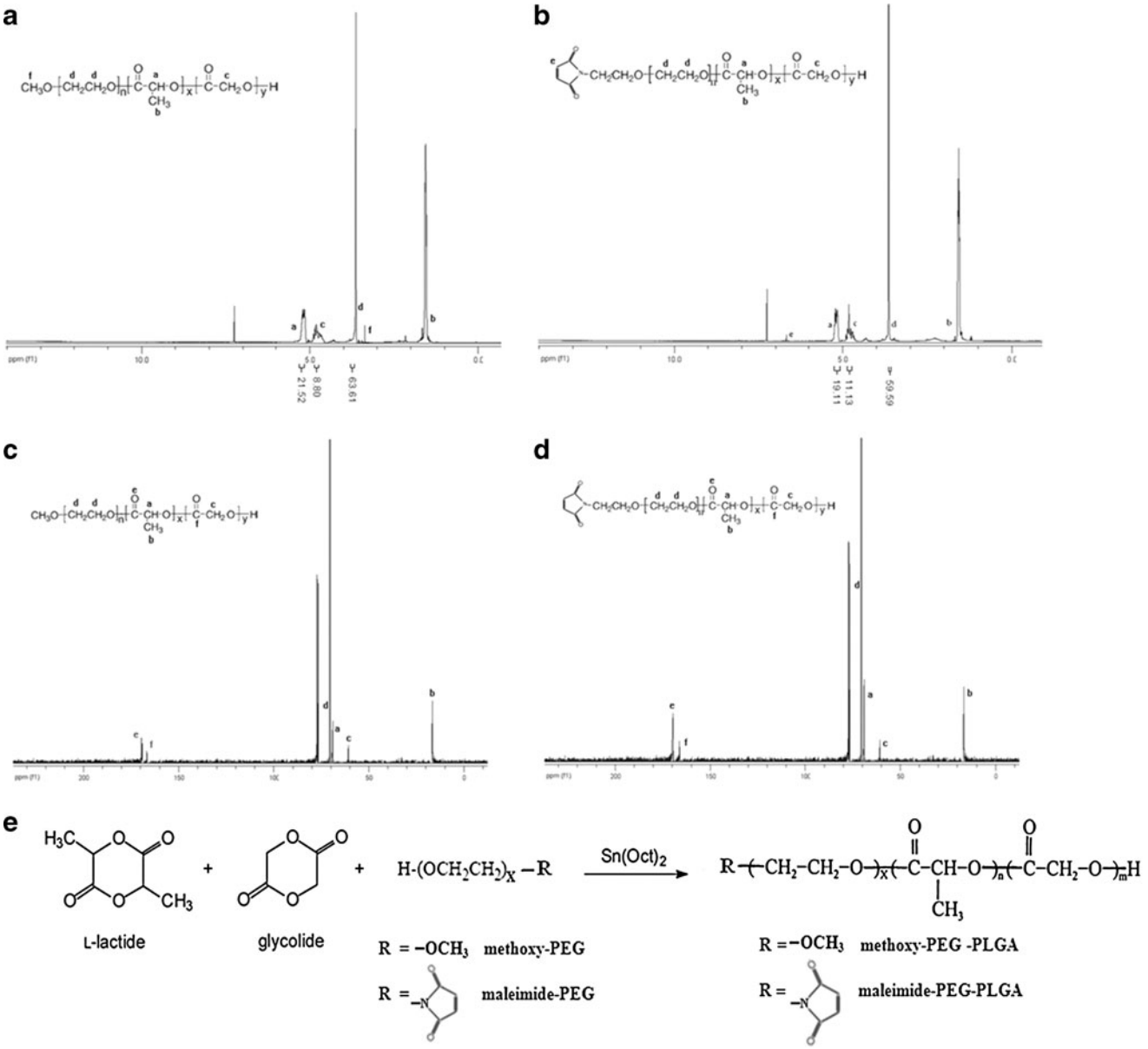

Fig. 1 ^{1}H-NMR and ^{13}C-NMR spectrum of the copolymer. (**a**) ^{1}H NMR spectrum of methoxy-PEG-PLGA. (**b**) ^{1}H NMR spectrum of maleimide-PEG-PLGA. (**c**) ^{13}C NMR spectrum of methoxy-PEG-PLGA. (**d**) ^{13}C NMR spectrum of maleimide-PEG-PLGA. (**e**) Chemical reactions for the prepartion of PEG-PLGA.

quantitative test. Examination showed that, *in vitro*, less than 0.6% of the 6-coumarin was released from the polymersomes in pH 7.4 PBS and 4.0 PBS after 72 h, indicating the 6-coumarin is an accurate and pH-dependent fluorescent probe (Fig. 3a).

In the present study, S14G-humanin was actively encapsulated into polymersomes by using a $(NH_4)_2SO_4$ ion gradient method. 1, 4-dioxane, was used to increase the membrane permeability and thus increased the drug loading. The DLE of the polymersomes is listed in Table I. The encapsulation process resulted in a total drug load of 0.77% of S14G-humanin (w/w) inside the polymersomes with an encapsulation efficiency of 21.78%. Within 12 h, the cumulative release percentage of drugs was 70% into PBS (pH 7.4) (Fig. 3b).

Surface Analysis

The chemical composition percents of carbon, oxygen, and nitrogen on the surface of the samples are given in Table II. Typical XPS survey scans are illustrated in Fig. 4. The nitrogen element was only detected in the Lf-POS sample and had a value of 0.84%. The peaks at binding energies of 280–305, 528–548, and 396–416 eV were ascribed to the

Table I Characteristics of Lf-POS Loaded with Either 6-Coumarin or S14G-Humanin

	Vesicle size (Mean±SD, nm)	Zeta potential (Mean±SD, mV)	DLE (Mean±SD,%)
Polymersomes	82.2±8.7	-4.42±0.12	
Lf_{59}-POS	85.2±8.5	-3.74±0.08	
Lf_{101}-POS	113.5±12.2	-3.89±0.12	
Lf_{268}-POS	136.7±11.5	-4.02±0.03	
6-coumarin-POS	108.2±9.5	-4.45±0.05	0.26±0.11
6-coumarin-Lf_{59}-POS	85.8±10.6	-3.28±0.15	0.22±0.09
6-coumarin-Lf_{101}-POS	115.6±10.3	-3.32±0.08	0.24±0.08
6-coumarin-Lf_{263}-POS	139.1±11.5	-3.33±0.16	0.27±0.05
SHN-Lf_{101}-POS	126.7±20.4	-2.54±0.05	0.77±0.02

elements of C1s, O1s, and N1s. The envelope fit for the C1s regions was presented using four main peaks: peak 1 corresponded to C–C/C–H (285 eV), peak 4 corresponded to O = C-C*(-C)-O (287.1 eV), peak 3 corresponded to O-C = O (289.2 eV) and peak 2 corresponded to C-O-C (286.5 eV) respectively (Fig.4a-c). The envelope fit for the O1s regions was presented using peaks corresponding to the two types of oxygen O = C (peak5, 532.4 eV) and O–C (peak6, 533.6 eV) (Fig. 4d-f). Peak 7 corresponded to the N1s envelope at 399.1 eV with a low signal (Fig. 4i). The chemical composition percents of carbon, oxygen, and nitrogen on the surface of the Lf-POS were 60.9%, 38.2%, and 0.84%, respectively. Those on the surface of the POS were 64.3%, 35.7%, and 0%, respectively (Table II). According to the chemical structures, the nitrogen element was attributed to the maleimide group of maleimide-PEG-PLGA and lactoferrin. A scan of the nitrogen failed to find the existence of N1s in both the maleimide-PEG-PLGA: methoxy-PEG–PLGA copolymers mixture (Fig. 4g) and the POS(Fig. 4h), suggesting that the nitrogen contribution of the maleimide group in XPS can be ignored. Peak 2, at the binding energy 286.5 eV, is regarded as the indicator of PEG, and can also be confirmed by an increased C-O-C peak ratio of 20.5% and 25.1% of POS and Lf-POS, respectively, compared with the maleimide-PEG–PLGA: methoxy-PEG-PLGA copolymers mixture (16.4%). This suggested that the PEG "corona" layer existed on the surface of the polymersomes.

CD68 Immunoexpression

The immunohistochemical staining showed there was no CD68 positive staining in the cerebrum (Fig. 5b,c) and cerebellum (Fig. 5e,f) following 7 days of continuous i.v. administration of Lf-POS, at a daily dose of 150 mg/kg. There was no significant difference when compared to the negative control (Fig. 5a, d). Immunohistochemistry of the liver of mice initially showed an increased amount of positive staining in Kupffer cells after 24 h (Fig. 5n), but this rapidly decreased to normal status after 72 h (Fig. 5o) as compared with the negative control. The same phenomenon occurred in both the spleen and kidney of mice, which illustrated that an excessive dose of Lf-POS caused a mild inflammatory reaction that was transient in these organs. The positive staining of macrophages in the spleen marginal zone increased (Fig. 5q) and then decreased to normal status after 72 h (Fig. 5r). The CD68 positive staining occurred in the mesangial cells of the renal corpuscle and decreased rapidly to normal status after 72 h, as compared with negative control (Fig. 5u). The negative staining of cardiac muscles in the heart (Fig. 5h,i) and dust cells in the lung (Fig. 5k,l) all showed no inflammation. In conclusion, a mild and transient inflammatory reaction appeared in the liver, spleen and kidney following a 7-day continuous intravenous administration of Lf -POS at daily dose of 150 mg/kg. However, there was no inflammatory reaction observed in the cerebrum, cerebellum, heart or lung.

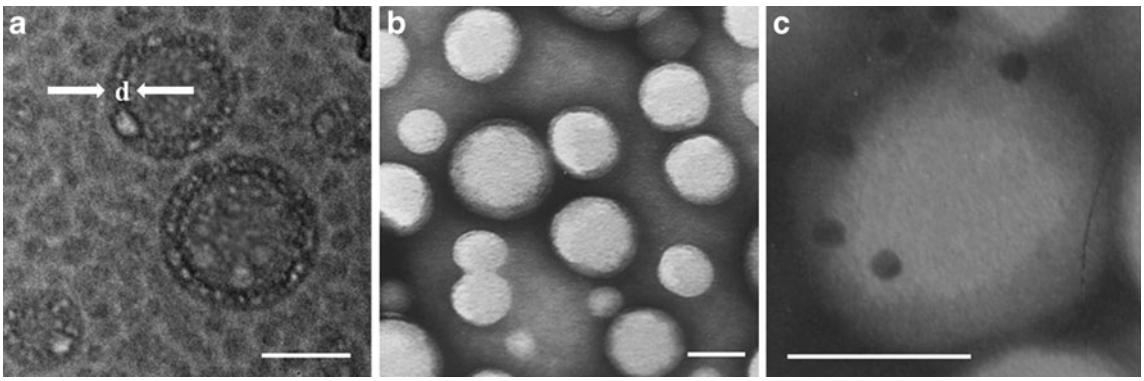

Fig. 2 (**a**) Images of Lf-POS by Cryo-TEM. (**b**) Images of Lf-POS by TEM. (**c**) TEM images of Lf-POS stained with goat-anti-mouse IgG-gold (10 nm). (bar 100 nm) (d was the membrane thickness of polymersomes).

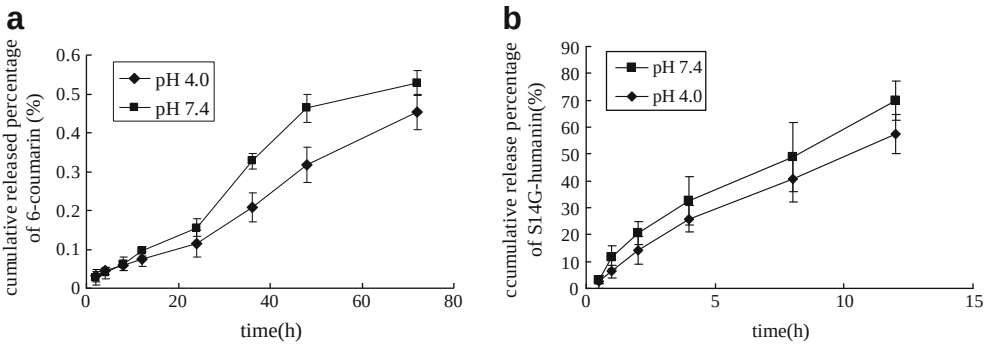

Fig. 3 *In vitro* release of 6-coumarin (**a**) and S14G-humanin (**b**) from polymersomes in PBS. (-■- pH 7.4, -▲- pH 4.0).

In Vivo Pharmacokinetics and Tissue Distribution of Lf-POS Loaded with 6-coumarin

In order to investigate the brain transport properties of Lf-POS associated with different lactoferrin densities on the surface, pharmacokinetic parameters and brain delivery properties were examined in mice after i.v. injection of 6-coumarin-loaded Lf-POS. Three different lactoferrin densities were tested, each at a dose of 5 mg/kg: 6-coumarin-Lf_{59}-POS, 6-coumarin-Lf_{101}-POS and 6-coumarin-Lf_{268}-POS. The permeability surface area (*PS*) product of 6-coumarin-Lf_{101}-POS (Fig. 6c) was 0.176 ml/h/g. The highest *PS* value and cumulation in brain tissue was obtained from this group (Fig. 6b). The brain tissue % ID/g for 6-coumarin-Lf_{101}-POS was 0.66%, which was 3.32-fold higher, as compared with 6-coumarin-POS($p<0.05$) (Fig. 6a). The decrease tendency of lactoferrin conjugated per polymersomes induced an increase in plasma clearance. When lactoferrin densities on the surface of the POS increased from 0 to 101, $AUC_{0\text{-}1h}$, *PS* and%ID/g also increased (Fig. 6a–c). However, at the highest lactoferrin densities, 6-coumarin-Lf_{268}-POS, a saturation effect was observed resulting in reduced brain tissue accumulation, in which $AUC_{0\text{-}1h}$,%ID/g, *PS* were lower than 6-coumarin-Lf_{101}-POS and V_D was increased(Fig. 6d).

Except for brain tissue, some main organs (heart, liver, spleen, lung and kidney) were collected and analyzed to obtain tissue uptake (%ID/g) after administration of Lf-POS with lactoferrin densities from 0 to 268 (Fig. 7). The highest tissue uptake was observed in the liver of mice. As the lactoferrin densities increased, the tissue uptake of the liver significantly increased. The % ID/g of 6-coumarin-Lf_{268}-POS was 3.12-fold higher than that of 6-coumarin-POS in liver of mice. Similar uptake trends were observed in the lung, where the % ID/g of 6-coumarin-Lf_{268}-POS increased 3.27-fold compared to 6-coumarin-POS (Fig. 7).

Immunohistochemical Analysis of Lf-POS Loaded with S14G-humanin

To investigate the effects of Lf-POS loaded with S14G-humanin (SHN-Lf_{101}-POS) on the neuron apoptosis-related protein and cholinergic system against the insult by amyloid-$\beta_{25\text{-}35}$, we carried out immunohistochemical analysis with anti-Bax polyclonal antibody, anti-caspase3 polyclonal antibody and anti-choline acetyltransferase polyclonal antibody in rat brains. The immunohistochemical staining results are shown in Fig. 8. A large number of ChAT positive cells existed in hippocampuses for the sham controls (Fig. 8a). Amyloid-$\beta_{25\text{-}35}$ administration caused a decrease in ChAT positive cells (Fig. 8b), while SHN-Lf_{101}-POS prevented this decrease (Fig.8c). From the results, it could be seen that overexpression of Bax (Fig. 8e) and caspase-3 (Fig. 8h) in hippocampal neuron cells was different from the sham controls. SHN-Lf_{101}-POS administration remarkably

Table II X-ray Photoelectron Spectroscopy (XPS) Analysis of Maleimide-PEG-PLGA: Methoxy-PEG-PLGA Mixture (1:5), POS (Maleimide-PEG-PLGA: Methoxy-PEG-PLGA Ratio is 1:5) Coupled with or without Lactoferrin (* Below the Detection Limit)

Samples	Elemental ratio (%)			C1s envelope ratios (%)			O1s envelope ratios (%)		
	C	O	N	C-C/C-H	C-O-C	O = C-C*(-C)-O	O-C = O	O = C	O-C
				Binding energy (eV)					
				285	286.5	287.1	289.2	532.4	533.6
copolymer	64.8	35.2	*	50.3	16.4	18.9	14.5	43.7	56.3
POS	64.3	35.7	*	50.1	20.5	18.6	14.9	47.5	52.5
Lf-POS	60.9	38.2	0.84	45.5	25.1	15.8	13.6	41.7	58.3

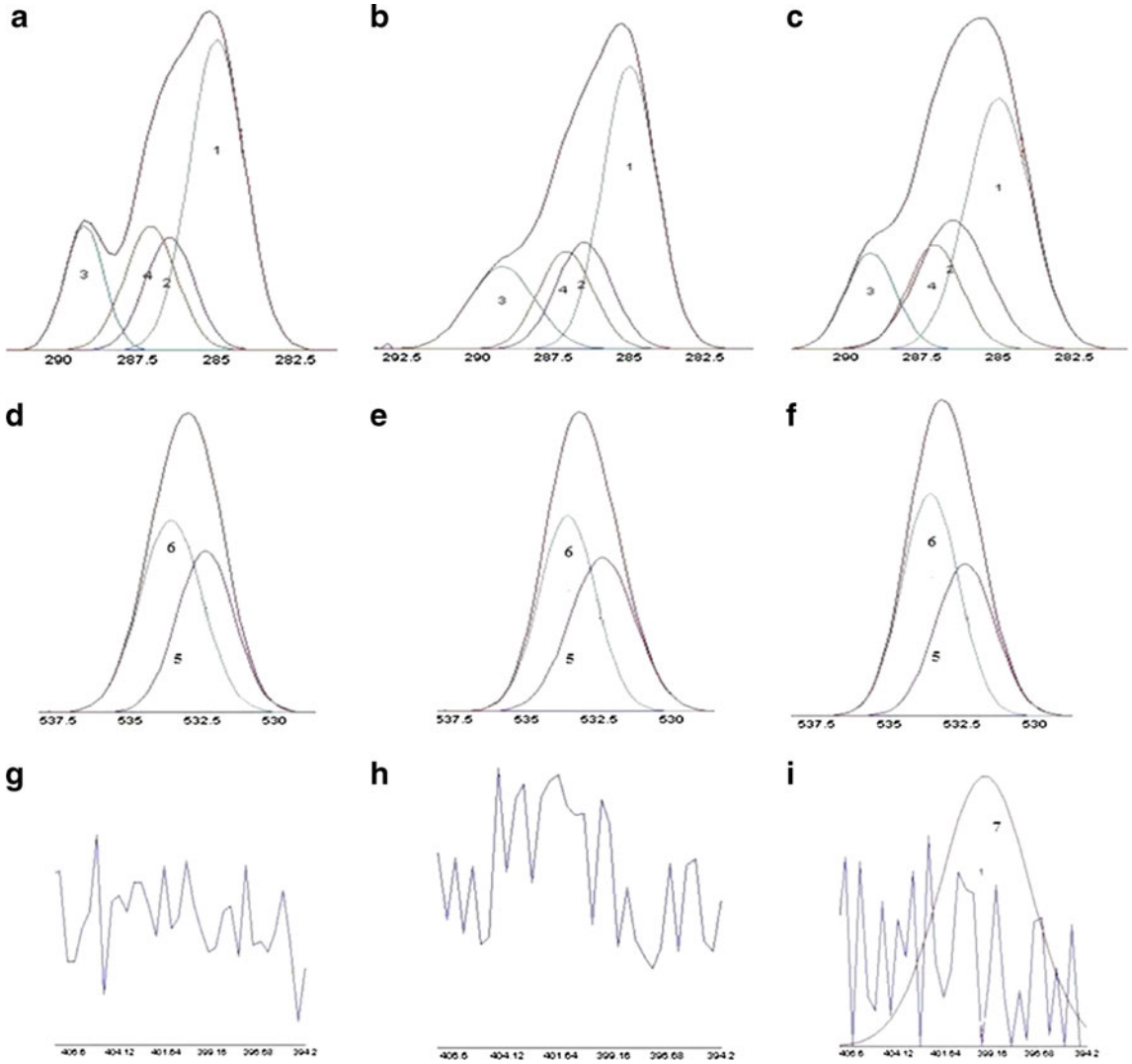

Fig. 4 X-ray photoelectron spectroscopy (XPS) analysis. Carbon C1s envelopes: (**a**) mixture of maleimide-PEG-PLGA: maleimide-PEG-PLGA mixture (1:5) copolymers; (**b**) POS, polymersomes unconjugated with lactoferrin; (**c**) Lf-POS (maleimide-PEG-PLGA: maleimide-PEG-PLGA ratio is 1:5). Oxygen O1s envelopes: (**d**) mixture of copolymers; (**e**) POS; (**f**) Lf-POS. Nitrogen envelopes: (**g**) mixture of copolymers; (**h**) POS; **i** Lf-POS.

attenuated the observed decrease in expression of Bax (Fig. 8f) and caspase-3 (Fig. 8i) positive cells in the hippocampal regions. The efficient inhibition of SHN-Lf_{101}-POS on amyloid-$\beta_{25\text{-}35}$-induced apoptotic proteins indicated that the nanocarrier system maintained a good brain targeting property.

DISCUSSION

Characterisics of Polymersomes

The diameter of the Lf-POS was approximately 120 nm, and the zeta potential was approximately -4 mV. The PEG chain, situated on the surface of the Lf-POS, can shield the negative charge produced by the central part of Lf-POS. Additionally, the weak positive charge on the lactoferrin molecule can bind to the negative charge on the membrane to enhance cellular uptake. Therefore, the Lf-POS maintains good properties as a particle which can meet the demands of brain drug delivery. Discher *et al.* considered that when the volume fraction ($f_{hydrophilic}$) between the hydrophilic fragment of an amphiphilic polymer and the whole molecule ranged from 0.20—0.42, a POS structure could come into being. (16). As a kind of supramolecular aggregate, the configuration and structure of POS has been studied, but it is not utilized exptensively as a drug carrier. We had previously conducted serial studies on POS. Pang *et al.* (36) demonstrated that POS prepared by PCL maintained a good cerebral property when mediated by OX26, which could inhibit the growth of rat glioma after intravenous injection, suggesting the feasibility of POS as a new brain drug delivery system.

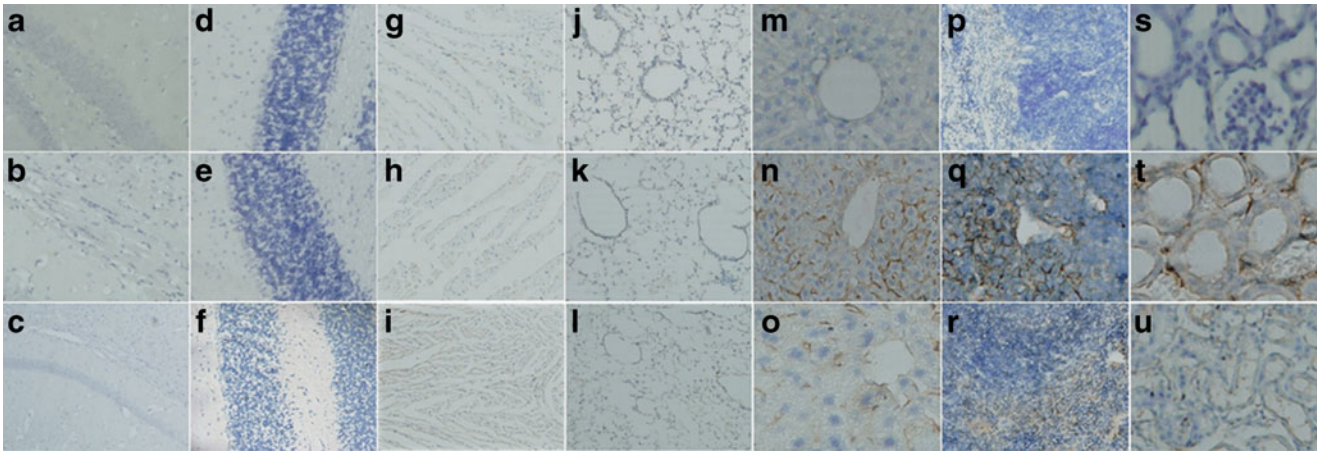

Fig. 5 Immunohistochemical staining of tissues of BALB/c mice showing CD68 immunoexpression after 7 days of continuous i.v. administration of 150 mg/kg/day Lf-POS. Negative staining is shown in cerebrum and cerebellum: 24 h (**b**, **e**) and 72 h (**c**, **f**) compared with negative control (**a**, **d**). Negative staining is shown in the cardiac muscles of the heart and dust cells of the lung: 24 h (**h**, **k**) and 72 h (**i**, **l**) compared with negative control (**g**, **j**). Positive staining of the hepatic lobule of the liver shows an increase in the amount of Kupffer cells at 24 h (**n**), and that the amount rapidly decreased after 72 h (**o**) compared with negative control (**m**). Positive staining of the spleen shows the increase of macrophages in the marginal zone at 24 h (**q**), and the rapid decrease after 72 h (**r**) compared with negative control (**p**). Positive staining of the renal corpuscle shows a significant increase of mesangial cells at 24 h (**t**), and the rapid decrease after 72 h (**u**) compared with negative control (**s**).

We chose biodegradable PLGA to synthesize a diblock copolymer by binding the hydrophilic methoxy-PEG and maleimide-PEG where the ratio of molecular weights was 9,042: 3,000 and 10,180: 3,500, respectively. The prepared POS had an inner structure made up of the hydrophobic fragments of the copolymer and a surface covered with hydrophilic PEG which could protect POS from being inactivated by mononuclear phagocyte systems. Since the lactoferrin on the surface of POS had to covalently bond with maleimide-PEG, the molecular weight of maleimide-PEG should be larger than that of methoxy-PEG. In this way, maleimide-PEG on the surface of the Lf-POS could stretch out to form a "brush-like" structure which would help the molecule covalently bond to lactoferrin. The lactoferrin binding to Lf-POS would be stretched out of the surface, in favor of the binding with LfR on BBB, before they were transported into the brain through receptor-mediated cytophagy.

Because POS is compatible with the biomembrane and has a water-soluble intracavity, we chose polymersomes as a carrier to encapsulate S14G-humanin. Due to its weak amphoteric but slight alkaline property, S14G-humanin

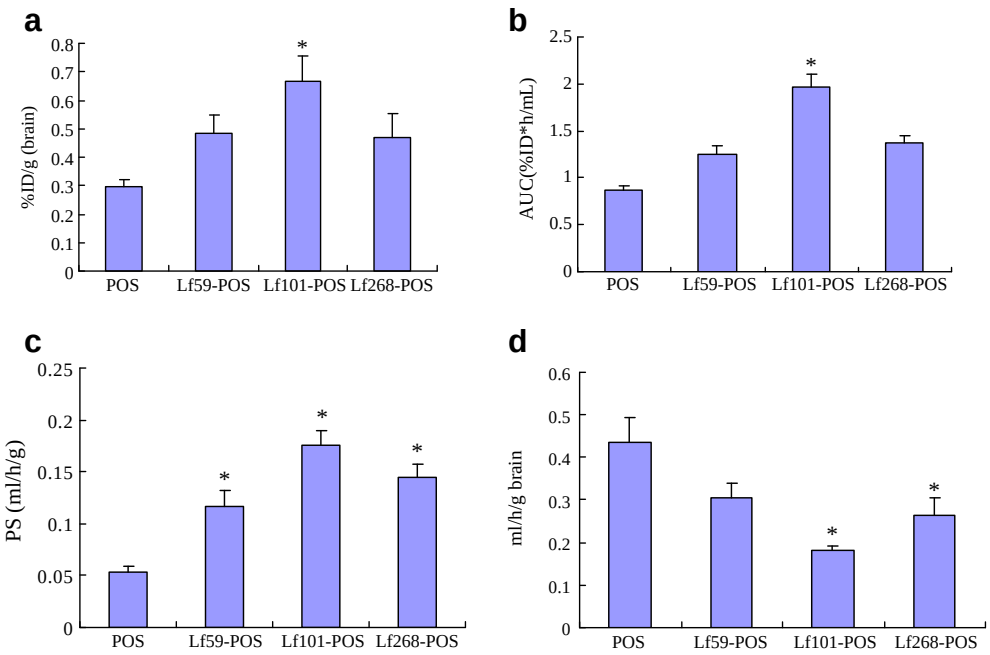

Fig. 6 Pharmacokinetic parameters and brain transport properties of 5 mg/kg Lf-POS loaded 6-coumarin with different lactoferrin densities per polymersomes (59, 101, 268) after i.v. ($n = 5$). *$p < 0.05$ Values apply to differences as compared to the POS control group. (**a**) % ID/g brain; (**b**) % ID/g brain; (**c**) *PS;* (**d**) V_D.

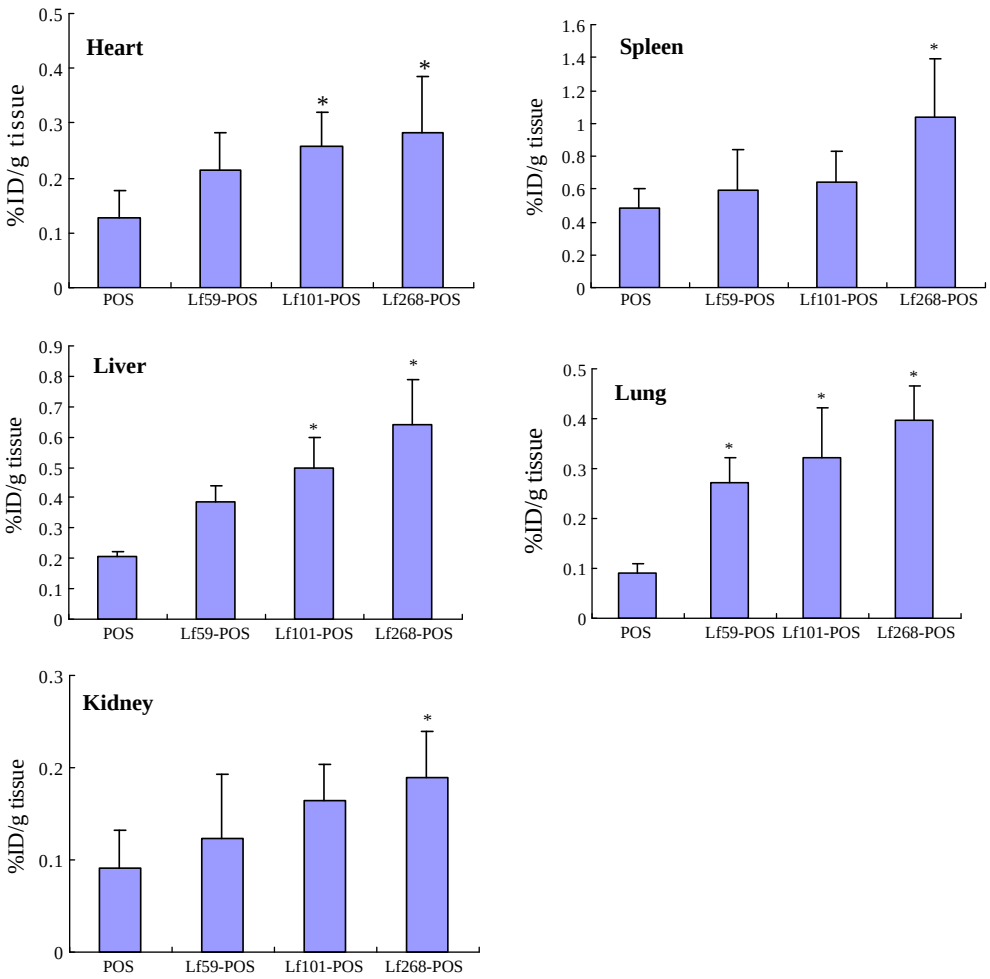

Fig. 7 Tissue uptake (% ID/g tissue) of Lf-POS-loaded 6-coumarin with different lactoferrin densities (0, 59, 101, 268) in mice after i.v. ($n = 5$). * $p < 0.05$values apply to differences as compared to the POS control group.

was actively encapsulated by using a $(NH_4)_2SO4$ ion gradient method. The 1, 4-dioxane, which can increase the flexibility of the membrane, was also added and improved the encapsulating rate from 5% to 21%. (24). The 1, 4-dioxane could reduce the viscosity of POS and enhance the permeability of the membrane and thus favor the transmembrane transport of the drug.

Optimization Densities of Lactoferrin Conjugated per Polymersomes

It has been reported that some receptors present on the cerebral microvascular endothelial membrane, such as transferrin, insulin or LDL receptors, can bind to the correlated ligands or monoclonal antibodies to mediate the entry of these ligands, antibodies or ligand/antibody modified drug delivery system into the brain (35). As previously reported (11), a cerebral lactoferrin receptor (LfR) had at least two types of binding sites. Since the endogenous lactoferrin was approximately 5 nmol/l, lower than the higher binding constant of the receptor, it could not bind to a vast number of LfR and competitively inhibit the drug delivery system modified by exogenous lactoferrin. This is an advantage of using lactoferrin as a brain targeting ligand.

It was shown that the brain delivery property of nanoparticles was affected by several physiochemical parameters, including size, ionic charge and surface characteristics (3,25). The emphasis on surface characteristics of Lf-POS in this work focused on lactoferrin densities. Our results showed that the brain distribution (% ID/g brain) of Lf-POS was not proportional to the surface densities of lactoferrin per polymersomes. The blood clearance of the POS also increased, and this caused a decrease in blood AUC. For this reason, the decreasing blood AUC was offsetting for the nominal increase of % ID/g. On the contrary, the hydrophilic PEG layer may disturb the interaction of the Lf-POS with the cells. If the surface PEG is increased, the BBB *PS* product may be decreased. However, the PEG shielding effect can prolong the circulation time of polymersomes in blood and increase its blood AUC compared with Lf-POS. In our study, the greatest %ID/g of brain tissue was observed for Lf_{101}-POS, a 2.23-fold increase as compared with POS alone. The *in*

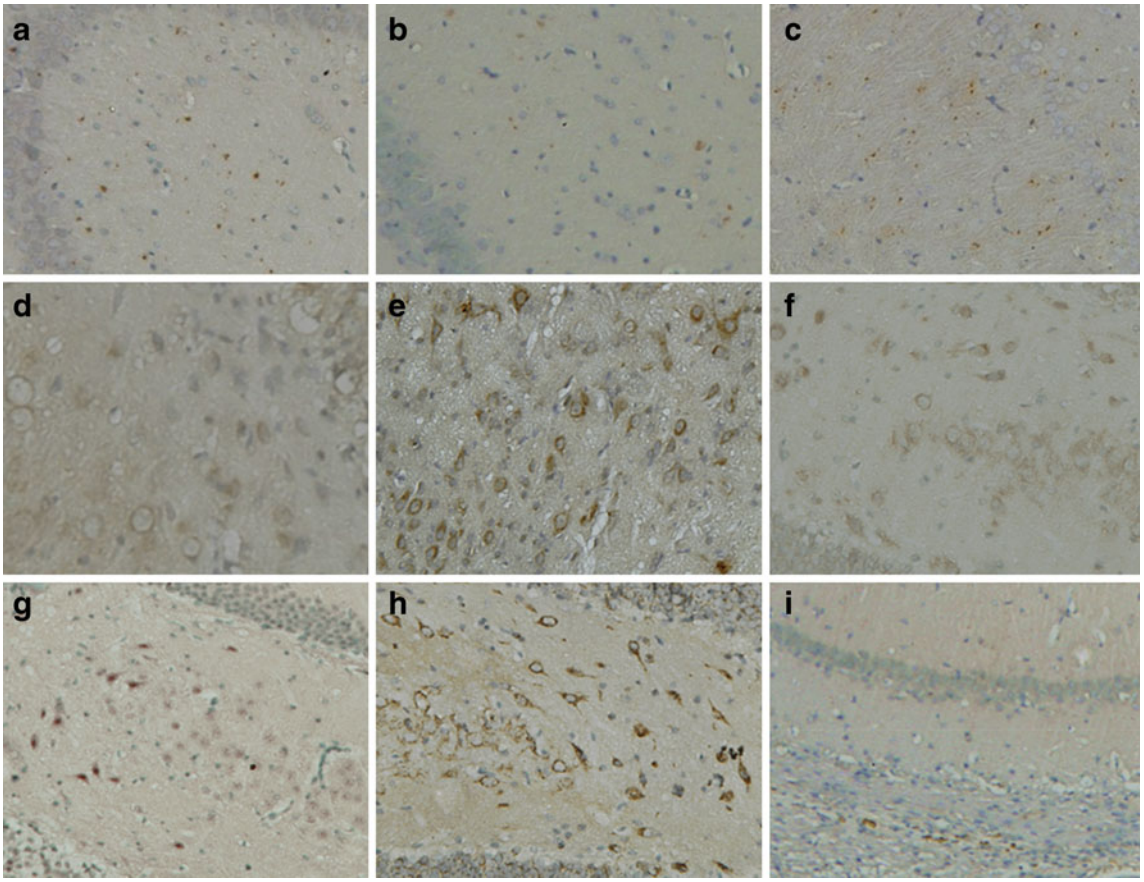

Fig. 8 The SHN-Lf_{101}-POS inhibited the over-expression of bax protein (**d**, **e**, **f**) and caspase-3 (**g**, **h**, **i**) and prevented reduction in ChAT (**a**, **b**, **c**). Activity on the rats induced by Amyloid-$\beta_{25\text{-}35}$ was identified by immunohistochemistry staining. (**a**, **d**, **g**) For the sham control group, saline was injected into the bilateral hippocampuses instead of Amyloid-$\beta_{25\text{-}35}$. (**a**, **d**, **g**). For the negative control group, administration of saline. (**c**, **f**, **I**) For the experimental group, administration of Lf_{101}-POS-loaded S14G-humanin at the dose of 25 μg/kg.

vivo brain delivery study demonstrated that the lactoferrin densities on the surface of polymersomes was positively correlated to the active targeting efficacy. However, the brain uptake of the drug delivery system did not increase over time due to the receptor saturation. When the lactoferrin densities reached a certain level, the uptake dose-effect features were no longer obvious. This suggested that only a certain range of lactoferrin densities determined the uptake of brain. The optimized lactoferrin number conjugated per polymersome was 101.

The Neuroprotective Effect of Lf-POS Loaded with S14G-humanin

The neuropathological manifestation of AD includes senile plaques, neurofibrillary tangles, amyloid vascular lesions and a loss of synapses and neurons. Nittaa *et al.* demonstrated that intracerebral amyloid-β administration could be used to establish an AD model in rats (37). Intracerebral amyloid-β sedimentation is associated with the degeneration of acetylcholine neurons and learning and memory impairment. A toxic fragment of amyloid-β, Amyloid-$\beta_{25\text{-}35}$, shows a neurotoxic effect on hippocampal neurons during primary culturing and could be directly injected into the hippocampuses of rats to simulate the behavioral and pathological changes of AD (33,34). Among the proteins associated with AD, Bax is an apoptotic promoter, and caspase-3 is an apoptosis-related protease. Previous studies indicated that Bax was found to be concentrated in senile plaques in the AD hippocampuses, which may be related to amyloid-β toxicity in AD brains, as well as tangles and astrocytes, indicating that Bax may play a role in the pathogenesis of AD (38,39). Caspase-3 activation is a pathological event that may be responsible for the loss of a subset of pyramidal neurons. Grosso *et al.* (40) hypothesized that caspase activation may occur as an early event initiated by a metabolic decline that precedes phosphorylation of neurofilaments and microtubules associated with the protein tau. Within the amyloid-β sequence, Amyloid-$\beta_{25\text{-}35}$ presented a strong neurotoxic effect. It was revealed that injecting Amyloid-$\beta_{25\text{-}35}$ into rat amygdalas could up-regulate Bax expression, which would then trigger the

apoptosis of neurons and make the rats show pathological changes similar to AD. S14G-humanin can effectively inhibit Bax (41) and caspase-3-dependent neuron apoptosis. It was previously reported that acetylcholine was deficient in AD patient brain tissues, especially in hippocampuses and temporal cortex (42). As shown in our study, SHN-Lf_{101}-POS had a protective effect on neurons by inhibiting the overexpression of Bax and caspase-3 as well as enhancing the activity of cholinesterase. All these findings indicate that Lf-mediated polymersomes as a novel drug carrier could efficiently mediate the active brain targeting

CONCLUSION

A novel brain drug delivery system, based on biodegradable PEG-PLGA polymersomes conjugated with lactoferrin, was developed and showed promising brain-targeting properties. The coupling of lactoferrin with polymersomes was examined by an immune colloidal gold technique and XPS examination. Pharmacokinetic profiles from this study suggest that the highest BBB permeability surface area product (*PS*) and percentage of injected dose per gram brain (% ID/g brain) were acquired by optimizing the surface lactoferrin densities on polymersomes. The optimized lactoferrin number conjugated per polymersomes was 101. Furthermore, Lf-POS-loaded S14G-humanin peptides provided a protective effect on rat hippocampal neurons treated with Amyloid-$\beta_{25\text{-}35}$. SHN-Lf_{101}-POS administration remarkably attenuated the expression of Bax and caspase-3 positive cells. Meanwhile, the activity of ChAT was increased compared with negative controls. These results indicate that Lf_{101}-POS is a promising brain drug delivery carrier, especially for peptide drugs across the BBB to the CNS.

ACKNOWLEDGMENTS & DISCLOSURES

This work was supported by National Basic Research Program of China (973 Program 2007CB935800), National Science and Technology Major Project (2009ZX09310-006), National Natural Science Foundation of China (30762544), and Postdoctoral Science Foundation of China (20060390144). The authors acknowledge Dr. Kunpeng Li, School of Life Sciences, Zhongshan University, China, for his precious help on Cryo-TEM of polymersomes.

REFERENCES

1. Huynh GH, Deen DF, Szoka Jr FC. Barriers to carrier mediated drug and gene delivery to brain tumors. J Control Release. 2006;110:236–59.
2. Cornford EM, Cornford ME. New systems for delivery of drugs to the brain in neurological disease. Lancet Neurol. 2002;1:306–15.
3. Pardridge WM. Drug and gene targeting to the brain via blood–brain barrier receptor-mediated transport systems. International Congress Series. 2005;1277:49–62.
4. Smith QR. Carrier-mediated transport to enhance drug delivery to brain. International Congress Series. 2005;1277:63–74.
5. Spencer BJ, Verma IM. Targeted delivery of proteins across the blood–brain barrier. PNAS. 2007;104:7594–9.
6. Witt KA, Davis TP. CNS drug delivery: opioid peptides and the blood-brain barrier. AAPS J. 2006;8:76–88.
7. Visser CC, Voorwinden H, Crommelin DJA, Danhof M, Boer AG. Characterization and modulation of the transferrin receptor on brain capillary endothelial cells. Pharm Res. 2004;21:761–9.
8. Sarzehi S, Chamani J. Investigation on the interaction between tamoxifen and human holo-transferrin: determination of the binding mechanism by fluorescence quenching, resonance light scattering and circular dichroism methods. Int J Biol Macromol. 2010;47:558–69.
9. Chamani J, Vahedian-Movahed H, Saberi MR. Lomefloxacin promotes the interaction between human serum albumin and transferrin: a mechanistic insight into the emergence of the antibiotic's side effects. J Pharm Biomed Anal. 2011;55:114–24.
10. Boado RJ, Zhang YF, Zhang Y, Pardridge WM. Humanization of anti-human insulin receptor antibody for drug targeting across the human blood-brain barrier. Biotechnol Bioeng. 2007;96:381–91.
11. Suzuki YA, Lopez V, Lonnerdal B. Mammalian lactoferrin receptors: structure and function. Cell Mol Life Sci. 2005;22:2560–75.
12. Ji B, Maeda J, Makoto H, Higuchi M, Inoue K, Akita H, *et al.* Pharmacokinetics and brain uptake of lactoferrin in rats. Life Sci. 2006;78:851–5.
13. Kabanov AV, Gendelman HE. Nanomedicine in the diagnosis and therapy of neurodegenerative disorders. Prog Polym Sci. 2007;32:1054–82.
14. Modi G, Pillay V, Choonara YE, Ndesendo VM, du Toit LC, Naidoo D. Nanotechnological applications for the treatment of neurodegenerative disorders. Prog Neurobiol. 2009;88:272–85.
15. Pardridge WM. Molecular Trojan horses for blood–brain barrier drug delivery. Curr Opin Pharmacol. 2006;6:494–500.
16. Discher DE, Eisenberg A. Polymer vesicles. Science. 2002;297:967–73.
17. Meng FH, Engbers HMG, Feigen J. Biodegradable polymer vesicles as a basis for artificial cells: encapsulation, release and targeting. J Control Release. 2005;101:187–98.
18. Ahmed F, Discher DE. Self-porating polymersomes of PEG-PLA and PEG-PCl: hydrolysis triggered controlled release vesicles. J Control Release. 2004;96:37–53.
19. Ahmed F, Pakunlu RI, Brannan A, Bates F, Minko T, Discher DE. Biodegradable polymer vesicles loaded with both paclitaxel and doxorubicin permeate and shrink tumors, inducing apoptosis in proportion to accumulated drug. J Control Release. 2006;116:150–8.
20. Mamiya T, Ukai M. [Gly14]-Humanin improved the learning and memory impairment induced by scopolamine *in vivo*. Br J Pharmacol. 2001;134:1597–9.
21. Avgoustakis K. Pegylated poly(Lactide) and poly(Lactide-Co-Glycolide) nanoparticles: preparation, properties and possible applications in drug delivery. Curr Drug Deliv. 2004;1:321–33.
22. Abraham SA, Edwards K, Karlsson G, Hudon N, Mayer LD, Bally MB. An evaluation of transmembrane ion gradient-mediated encapsulation of topotecan within liposomes. J Control Release. 2004;96:449–61.
23. Choucair A, Soo PL, Eisenberg A. Active loading and tunable release of doxorubicin from block copolymer vesicles. Langmuir. 2005;21:9308–13.

24. Wu J, Eisenberg A. Proton diffusion across membranes of vesicles of poly(styrene-b-acrylic Acid) diblock copolymers. JACS. 2006;128:2880–4.
25. Huwyler J, Wu DF, Pardridge WM. Brain drug delivery of small molecules using immunoliposomes. PNAS. 1996;93:14164–9.
26. Lu W, Wan J, She ZJ, Jiang XG. Brain delivery property and accelerated blood clearance of cationic albumin conjugated pegylated nanoparticle. J Control Release. 2007;118:38–53.
27. Olivier JC, Huertas R, Lee HJ, Calon F, Pardridge WM. Synthesis of pegylated immunonanoparticles. Pharm Res. 2002;19:1137–43.
28. Taylor S, Brock J, Kruger C. Safety determination for the use of bovine milkderived lactoferrin as a component of an antimicrobial beef carcass spray. Regul Toxicol Pharm. 2004;39:12–24.
29. Shard AG, Davies MC, Li YX, Volland C, Kissel T. XPS and SSIMS analysis revealing surface segregation and short-range order in solid films of block copolymers of PEO and PLGA. Macromolecules. 1997;30:3051–7.
30. Novotná K, Havliš J, Havel J. Optimisation of high performance liquid chromatography separation of neuroprotective peptides: fractional experimental designs combined with artificial neural networks. J Chromatogr A. 2005;1096:50–7.
31. Thom SR, Bhopale VM, Fisher D, Zhang J, Gimotty P. Delayed neuropathology after carbon monoxide poisoning is immune-mediated. Proc Natl Acad Sci. 2004;101:13660–5.
32. Alric L, Orfila C, Carrere N, Beraud M, Carrera G, Lepert JC, *et al.* Reactive oxygen intermediates and eicosanoid production by kupffer cells and infiltrated macrophages in acute and chronic liver injury induced in rats by CCl_4. Inflamm Res. 2000;49:700–7.
33. Kim DH, Kim S, Jeon SJ, Son KH, Lee S, Yoon BH, *et al.* The effects of a-cute and repeated oroxylin a treatments on $A\beta_{25\text{-}35}$ induced memory impairment in mice. Neuropharmacology. 2008;55:639–47.
34. Tajima H, Kawasumi M, Chiba T, Yamada M, Yamashita K, Nawa M, *et al.* A humanin derivative, S14G-HN, prevents amyloid–induced memory impairment in mice. J Neurosci Res. 2005;79:714–23.
35. Pardridge WM. Molecular Trojan horses for blood–brain barrier drug delivery. Curr Opin Pharmacol. 2006;6:494–500.
36. Pang ZQ, Lu W, Gao HL, Hu KL, Chen J, Zhang CL, *et al.* Preparation and brain delivery property of biodegradable polymersomes conjugated with OX26. J Control Release. 2008;128:120–7.
37. Nittaa A, Itoha A, Hasegawaa T, Nabeshima T. β-Amyloid protein-induced Alzheimer's disease animal model. Neurosci Lett. 1994;170:63–6.
38. Su JH, Deng G, Cotman CW. Bax protein expression is increased in Alzheimer's brain: correlations with DNA damage, Bcl-2 expression, and brain pathology. J Neuropath Exp Neur. 1997;56:86–93.
39. MacGibbon GA, Lawlor PA, Sirimanne ES, Walton MR, Connor B, Young D, *et al.* Bax expression in mammalian neurons undergoing apoptosis, and in Alzheimer's disease hippocampus. Brain Res. 1997;750:223–34.
40. Grossoa CA, Tamb J, Royb S, Xanthoudakisb S, Costaa DD, Nicholsonb DW, *et al.* Caspase-3 cleaved spectrin colocalizes with neurofilament-immunoreactive neurons in Alzheimer's disease. Neuroscience. 2006;141:863–74.
41. Guo B, Zhai DY, Cabezas E, Welsh K, Nouraini S, Satterthwait AC, *et al.* Humanin peptide suppresses apoptosis by interfering with Bax activation. Nature. 2003;423:456–61.
42. DeKosky ST, Ikonomovic MD, Styren SD, Beckett L, Wisniewski S, *et al.* Upregulation of choline acetyltransferase activity in hippocampus and frontal cortex of elderly subjects with mild cognitive impairment. Ann Neurol. 2002;51:145–5.